Hindawi
Journal of Nanomaterials
Volume 2017, Article ID 7431432, 6 pages
https://doi.org/10.1155/2017/7431432

Research Article

Study on the Effect of γ-Irradiation on Gadolinium Oxysulfide Nanophosphors (Gd_2O_2S-NPs)

Muhammad Hassyakirin Hasim, Irman Abdul Rahman, Sapizah Rahim, Muhammad Taqiyuddin Mawardi Ayob, Shamellia Sharin, and Shahidan Radiman

Nuclear Technology Research Centre, Faculty of Science and Technology, Universiti Kebangsaan Malaysia, 43600 Bangi, Selangor, Malaysia

Correspondence should be addressed to Irman Abdul Rahman; irman@ukm.edu.my

Received 6 March 2017; Revised 18 May 2017; Accepted 8 June 2017; Published 12 July 2017

Academic Editor: Stefano Bellucci

Gadolinium oxysulfide nanophosphors (Gd_2O_2S-NPs) have been successfully synthesized using γ-irradiation and hydrogenation treatment. The primary stage of Gd_2O_2S-NPs synthesis was carried out using various doses of γ-irradiation to form diverse sizes of $Gd_2(SO_4)_3$ precursor, followed by hydrogenation treatment at 900°C for 2 hours to form Gd_2O_2S-NPs. Then, the nanophosphors were characterized for the structure, morphology, and luminescence properties through X-ray diffraction (XRD), field emission scanning electron microscopy (FESEM), and photoluminescence spectrometer (PL). Pure hexagonal phase of Gd_2O_2S-NPs was obtained with high crystallinity and without any impurities. The morphologies were observed from grain-like nanostructures transformed to spherical shape as the irradiation dose reached 40 kGy. Besides, Gd_2O_2S-NPs which were prepared at highest irradiation dose of 40 kGy show highest intensity of emission peak at 548 nm and corresponded to Stark level transition from the ^6G_J state of Gd^{3+} ion. It can be emphasized that the different doses of γ-irradiation influenced the nucleation event of $Gd_2(SO_4)_3$ precursor thus affecting the morphology and size particles of Gd_2O_2S-NPs. Hence, from the results, it can be suggested that Gd_2O_2S-NPs can be a promising host for optical applications.

1. Introduction

In the last decade, lanthanide materials have displayed the potential to be utilized as efficient phosphors in many applications, such as solar energy converters [1], optical amplifiers [2], and thermoluminescent dosimeters [3]. Lanthanide materials can be fabricated into nanoscale materials which exhibit extraordinary properties in comparison to bulk materials, which is ideal for a wide range of applications. Therefore, gadolinium oxysulfide nanophosphors (Gd_2O_2S-NPs) were chosen due to its high chemical and thermal stability as well as wide band gap energy in the range of 4.6 to 4.8 eV, which is suitable for ionic doped activation [4] and efficiently reacted to become as a luminescent emitting material [5]. It has been deliberated as a host for optical activation with various numbers of rare earth ions to reveal different luminescence peaks of the activators [6]. From this point of view, Gd_2O_2S-NPs seem to display characteristics of a good host matrix for luminescent rare earth ions to fabricate phosphors. Furthermore, the high density of Gd_2O_2S-NPs (7.34 g/cm^3) makes it a suitable as a host for higher concentration of dopant [4]. Due to these remarkable features, this material is promising for various applications which includes radiographical applications and medical diagnostic, especially in charge-coupled device (CCD) camera for electron microscopy [7], ceramic scintillators [8], cathode ray tube (CRTs) [9], and multimodal imaging agent [10].

In terms of Gd_2O_2S-NPs synthesis, researchers have proposed several methods to synthesize these nanophosphors, including solvothermal method [11], coprecipitation method [12], microwave solid-state method [13], vacuum firing method [14], and microemulsion liquid method [15]. From the list above, none have utilized γ-irradiation to synthesize Gd_2O_2S-NPs. We chose to utilize γ-irradiation method in order to prepare Gd_2O_2S-NPs due to its simplicity, low cost, and chemical safety. Moreover, this method had

the ability to form Gd_2O_2S in nanometer scale with high purity and high stable state [16]. The formation of Gd_2O_2S-NPs would be attributed to the radiolysis process in aqueous solution that creates ionic radicals and reduces metal ions. In this study, when aqueous solutions were exposed to γ-rays, they create solvated electrons, which reduced gadolinium ions to form highly pure gadolinium metal, $Gd^{3+} \rightarrow Gd^0$. As a result, the particles size will also be reduced. To complete the synthesis, the hydrogenation treatment was adopted in the final stage of synthesis to reduce gadolinium oxysulfate ($Gd_2O_2SO_4$) to gadolinium oxysulfide (Gd_2O_2S) after completing the deoxygenation reaction. By controlling the concentration of surfactant and starting materials of the solutions, we performed these reactions under different radiation doses in order to study the effect of γ-irradiation on the physical and optical characteristics of the Gd_2O_2S-NPs such as morphology, crystallinity, particle size, and photoluminescence intensity.

Consequently, as the γ-irradiation method managed to control size and morphology particles of Gd_2O_2S-NPs at various doses, the growth mechanisms and photoluminescence properties of the Gd_2O_2S-NPs will be investigated and discussed in detail.

2. Experimental Details

2.1. Materials. Gadolinium (III) nitrate hexahydrate, $Gd(NO_3)_3{\cdot}6H_2O$ (99.9%), and cetyltrimethylammonium bromide, CTAB (≥98%) were purchased from Sigma-Aldrich. Ammonium sulfate $(NH_4)_2SO_4$ was purchased from Merck. All reagents were analytical grade and used without further purification.

2.2. Preparation of Gd_2O_2S-NPs. In a typical synthesis of the nanophosphors, the starting materials of $Gd(NO_3)_3{\cdot}6H_2O$ (20 mM) and CTAB (40 mM) were dissolved in deionized water. The mixture solution was stirred for an hour. Later, $(NH_4)_2SO_4$ (30 mM) solution was added dropwise into the solution mixture and stirred continuously overnight. In order to avoid oxidation due to the oxidizing species such as hydroxyl radical, 1 ml of isopropanol was added to each of the samples before irradiation treatment. The mixture was then portioned into five samples (0 kGy, 10 kGy, 20 kGy, 30 kGy, and 40 kGy) and irradiated with Cobalt-60 gamma source with a dose rate of 1.45 kGy/h under atmospheric pressure and room temperature. Meanwhile, the 0 kGy sample was used as a control. The solid precipitates were obtained via centrifugation (4000 rpm) before being purified and dried in air at ambient temperature overnight. Afterwards, the final products were obtained through a heat treatment at 900°C for 2 hours in the flow of hydrogen gas. Finally, after cooling down to room temperature, the Gd_2O_2S-NPs were obtained in powder form.

2.3. Characterization Techniques. The X-ray diffraction (XRD) measurements of Gd_2O_2S-NPs samples were carried out in the reflection mode with a Bruker X-ray diffractometer that operated at 40 kV voltages and a current of 40 mA with Cu Kα radiation (λ = 0.15406 nm). The continuous scanning rate, 2θ range from 20° to 80° used for phase formation determination, was $5^\circ\,(2\theta)\,\text{min}^{-1}$. The morphology and size of the samples were inspected by the field emission scanning electron microscopy (FESEM-Carl Zeiss, Supra 35VP) imaging. Meanwhile, the photoluminescence spectra of the samples were gathered over a range 400–800 nm via FLSP920 Edinburgh spectrometer.

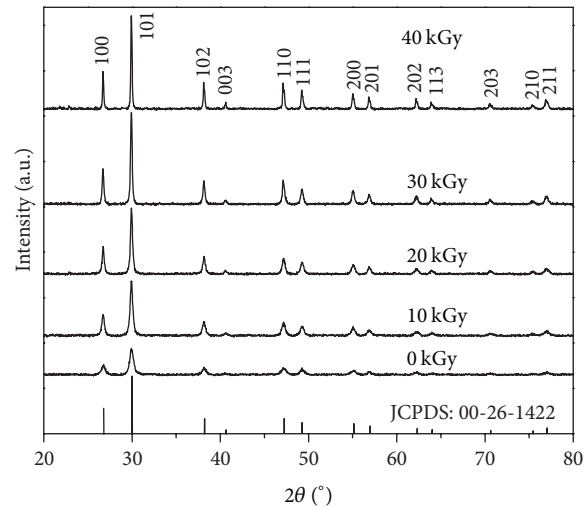

Figure 1: XRD patterns of Gd_2O_2S-NPs under different irradiation doses: 0 kGy, 10 kGy, 20 kGy, 30 kGy, and 40 kGy and standard file of Gd_2O_2S (JCPDS: 00-26-1422) for comparison.

3. Results and Discussion

3.1. X-Ray Diffraction Analysis. Figure 1 shows the XRD patterns of $Gd_2O_2S_2$-NPs at different irradiation doses. The diffraction peaks of all samples (0–40 kGy) were indexed as pure hexagonal phase and perfectly match the reference pattern of JCPDS card number 00-026-1422. As the irradiation doses were increases, the XRD patterns exhibit minimal changes but no other phase was produced. Apart from that, the sample irradiated with 40 kGy shows the best crystalline pattern with a strong and sharp diffraction peaks. The calculated lattice constants ($a = b$ = 3.853 Å, c = 6.665 Å) were similar to the hexagonal phase of Gd_2O_2S from reference data ($a = b$ = 3.852 Å, c = 6.665 Å). Thus, we can confirm that the pure oxysulfide phase was obtained without any impurities. In addition, the average crystallite sizes of particles were calculated using Scherrer's equation:

$$D_{h\,k\,l} = \frac{K\lambda}{\beta \cos\theta}, \tag{1}$$

where $D_{h\,k\,l}$ defines the size along the (h k l) direction and K is a constant (0.941), where θ and β are diffraction angle and full-width at half maximum (FWHM), respectively. The three strongest peaks at 2θ = 26.730° (100), 29.927° (101), and 38.138° (102) were used to calculate the average crystallite sizes (D) of the samples. Consequently, the average crystallite sizes were found to be in the range of 27 to 35 nm.

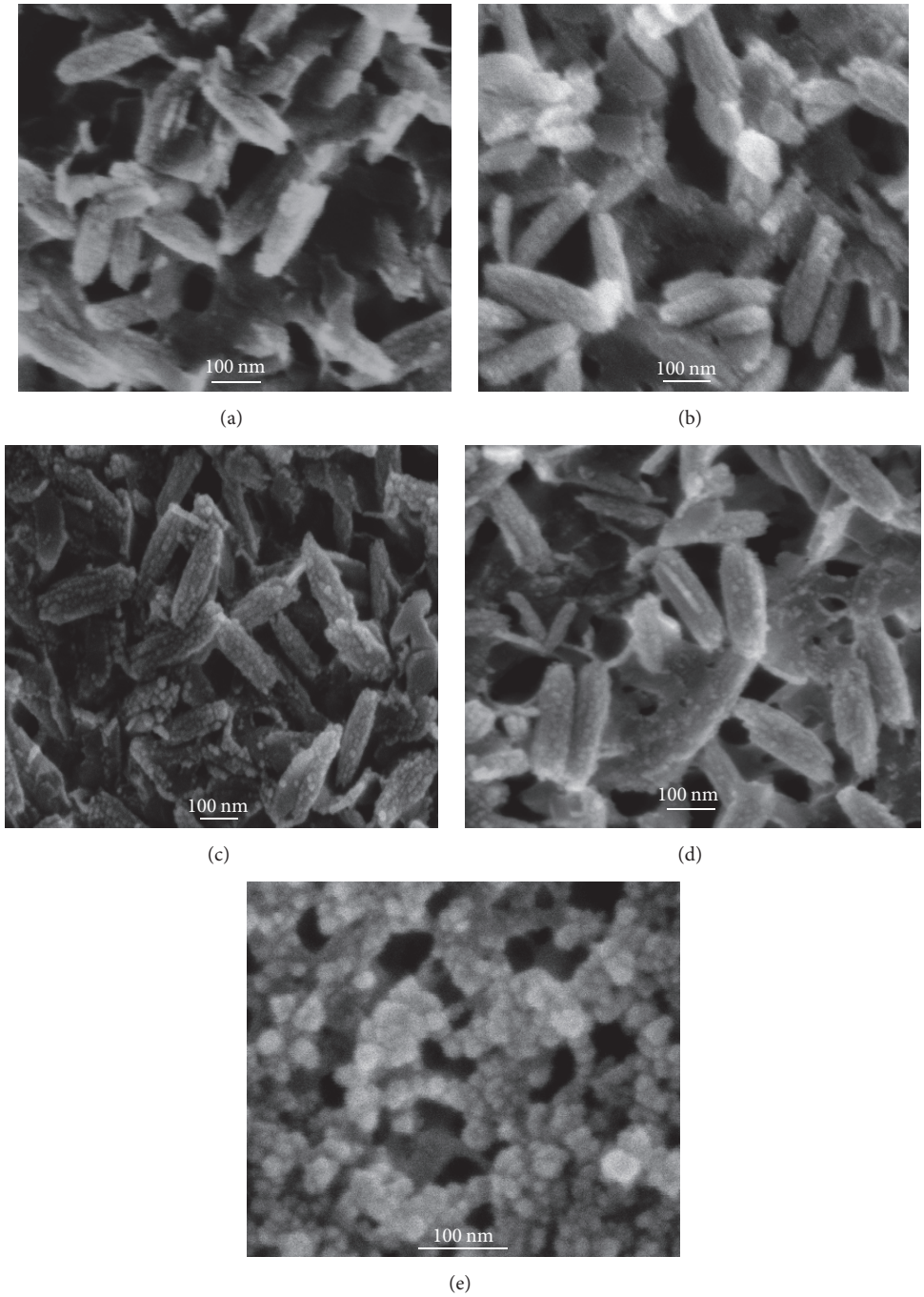

Figure 2: FESEM images of Gd_2O_2S-NPs by different irradiation doses: (a) 0 kGy, (b) 10 kGy, (c) 20 kGy, (d) 30 kGy, and (e) 40 kGy.

3.2. FESEM Analysis. The typical FESEM images of the produced Gd_2O_2S-NPs morphologies as shown in Figure 2 reveal that the product mainly consists of grain-like nanostructures which transformed into spherical shape as the irradiation dose reached 40 kGy. The grain-like nanostructures displayed a length × width of ~200 nm × 50 nm, meanwhile the spherical shape morphology displayed a diameter of 10 nm to 30 nm. The evolution of Gd_2O_2S-NPs morphology from grain-like to spherical was observed as the irradiation dose increases. Moreover, the sample with 40 kGy irradiated dose in Figure 2(e) shows a well dispersed surface of morphology compared to the other samples at lower doses (0–30 kGy). Therefore, the γ-irradiation could generated more defined structures and also homogeneous particles size distribution. It can be presumed that the morphological changes are a consequence of radical linkage and hydrated electron (e_{aq}^-) affecting the CTAB aqueous solution in certain path [17]. Thus, it forms a new capping layer on the Gd_2O_2S-NPs surfaces due to the structures modification of CTAB, resulting in the formation of the spherical shape of Gd_2O_2S-NPs, as

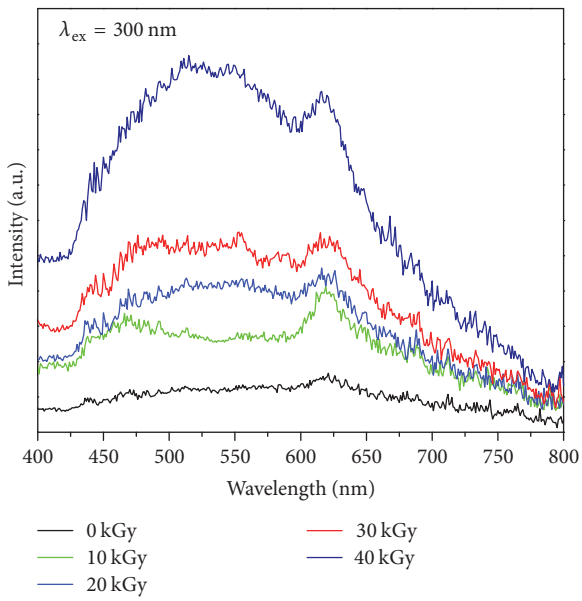

FIGURE 3: Emission spectra of Gd_2O_2S-NPs at various irradiation doses.

shown in Figure 2(e) [18]. Additionally, CTAB also plays an important role in limiting the growth of the particles shape by selectively or more strongly binding to various emerging crystal facets [18]. In this occasion, Gd_2O_2S-CTAB complex compound was formed. Due to this reason, the Gd_2O_2S particles evolved into a more defined shape [19]. At higher doses, the CTAB structures become more complex and inhibiting the aggregation of Gd_2O_2S-NPs by forming a thin layer of single particle which is well dispersed in the solution. Therefore, this explains the predominant formation of smaller and scattered Gd_2O_2S-NPs at higher doses as observed in Figure 2(e).

3.3. Mechanisms of Gd_2O_2S-NPs Formation. The morphology changes of Gd_2O_2S-NPs can be attributed to the radiolysis treatment in aqueous solutions that provides an efficient method to reduce metal ions [20]. Aqueous solutions containing isopropanol exposed to γ-irradiation lead to the formation of hydrated electrons (e_{aq}^-) and primary species H_3O^+, H_2, H^*, OH^*, and H_2O_2 (2) [16]. These free radicals may present a destructive effect to the CTAB structures resulting in separating of the cluster capped particles of Gd_2O_2S-NPs (Figure 2(a)) to single capped particles (Figure 2(e)). Equation (3) shows the reduction of primary ions, Gd^{3+} to neutral Gd^0, which have been formed during the primary reaction by dissociation of gadolinium nitrate and ammonium sulfate in DI water. Afterwards, ammonium nitrate ($(NH_4)(NO_3)$) and gadolinium sulfate ($Gd_2(SO_4)_3$) formed as products for the secondary reaction, as shown in (4).

$$H_2O \longrightarrow e_{aq}^-,\ H_3O^+,\ H_2,\ H^*,\ OH^*,\ H_2O_2 \quad (2)$$

$$Gd^{3+} + 3e_{aq}^- \longrightarrow Gd^0 \quad (3)$$

$$Gd(NO_3)_3 + (NH_4)_2SO_4 \longrightarrow Gd_2(SO_4)_3 + (NH_4)(NO_3) \quad (4)$$

During the radiolysis process, γ-irradiation increases the nucleus event of the precursors. At lower absorption doses, the nucleation event is lower than total ions; hence larger particles are obtained. Meanwhile, at higher absorption doses, the nucleation event is higher than total ions, thus creating smaller particles in the aqueous solution [16].

In order to complete the synthesis of Gd_2O_2S-NPs, hydrogenation process was applied. This process is considered the best approach to fabricate the nanophosphor into complete form, due to its straightforward process and nonutilization of toxic carbon disulfide (CS_2) or hydrogen sulfide (H_2S) [21]. As the temperature reached 700°C, the precursor of $Gd_2(SO_4)_3$ started to turn into $Gd_2O_2SO_4$ (5) due to oxygenation reaction from the calcinations process.

$$Gd_2(SO_4)_3 + O_2 \longrightarrow Gd_2O_2SO_4 \quad (5)$$

$$Gd_2O_2SO_4 + 4H_2 \longrightarrow Gd_2O_2S + 4H_2O \quad (6)$$

Afterwards, the precursor of $Gd_2O_2SO_4$ undergoes calcination at 900°C for 2 hours with the flow of hydrogen gas by placing the sample into tube furnace. Soon after, deoxygenation reaction has taken place by removing oxygen ion, O^{2-} from the $Gd_2O_2SO_4$ precursor (6) due to combination of the hydrogen gas, H_2 with the oxygen to form water, H_2O which becomes the excess product. Consequently, the desired final product of Gd_2O_2S-NPs was successfully obtained.

3.4. Photoluminescence Study. Gd_2O_2S-NPs have been known to be excellent host material as doping activation ion due to their own luminescence behaviour [22]. In order to confirm the existence of these properties, we carried out the photoluminescence measurements at room temperature under 300 nm UV excitation wavelength. The emission spectra of Gd_2O_2S-NPs at various irradiation doses are shown in Figure 3. It shows that the intensity of emission spectra significantly increases with the increasing of γ-irradiation dose. Therefore, the emission spectra of 40 kGy sample show the highest intensity peak located at 548 nm which corresponded to the green emission compared to the other doses. This green emission corresponded to the Stark level transition from the ^6G_J state of Gd^{3+} ion [23]. In addition, the red emission peak can also be seen at 621 nm, which is matching to the $^6G_J \rightarrow {}^6P_J$ transition [23].

The emission spectrum of the samples (0–40 kGy) does not exhibit strong and sharp peaks, but displays wide and broad peaks due to the absence of trivalent rare earth doping activation ion such as Europium ion (Eu^{3+}), Praseodymium ion (Pr^{3+}), and Terbium ion (Tb^{3+}) [24]. The absence of these doping activation ions ruled out the transition of emission between conduction band and valance band. This implicates that the weak emission either comes from deep-level or trap-state emission [25]. However, the 40 kGy still managed to produce high intensity and widened peak of emission spectra compared to the other samples. Meanwhile, for the samples at lower irradiation dose (0–30 kGy), the quenching

effect occurred on the photoluminescence spectrum. These phenomena appeared due to the large particles size and rough surface phase formations, as proven on the FESEM images (Figures 2(a)–2(d)). From the results formation of these particles, it can restrict the emission occurrence.

In conclusion, the crystallinity, lattice constant, and morphology will affect the surface state of particles in order to obtain well define energy band gap or excitonic emission [26]. It can be emphasized that the particles size distributions with spherical shaped of Gd_2O_2S-NPs may also play a major role in the emission origination.

4. Conclusion

In summary, the γ-irradiation method plays an important role in order to control the phase surface and morphology of Gd_2O_2S-NPs combining with a heat treatment process. The Gd_2O_2S-NPs obtained with hexagonal phase with no other phases introduced as the irradiation dose achieved 40 kGy. The photoluminescence studies show that the intensity of emission spectra also increases with increasing irradiation dose; this happened due to the particles size decrease homogeneously on the volume and surface. Hence, the γ-irradiation method not only has the advantages of simplicity, low cost, and chemical safety, but also has the ability to produce well dispersed and nanosized particles. We hope that this method will become a promising approach in order to synthesize good forms of the other nanophosphors in the future.

Conflicts of Interest

The authors have declared no financial conflicts of interest in this manuscript.

Acknowledgments

The authors wish to acknowledge MOE (FRGS/1/2014/SG06/UKM/02/3), UKM (AP-2015-006), UKM (DPP-2015-031), and UKM (GUP-2016) for their financial support. The authors also are grateful for the characterization support from CRIM, UKM.

References

[1] B. M. van der Ende, L. Aarts, and A. Meijerink, "Lanthanide ions as spectral converters for solar cells," *Physical Chemistry Chemical Physics*, vol. 11, no. 47, pp. 11081–11095, 2009.

[2] K. Kuriki, Y. Koike, and Y. Okamoto, "Plastic optical fiber lasers and amplifiers containing lanthanide complexes," *Chemical Reviews*, vol. 102, no. 6, pp. 2347–2356, 2002.

[3] K. S. V. Nambi, V. N. Bapat, and A. K. Ganguly, "Thermoluminescence of $CaSO_4$ doped with rare earths," *Journal of Physics C: Solid State Physics*, vol. 7, no. 23, pp. 4403–4415, 1974.

[4] J. Lian, X. Sun, T. Gao, Q. Li, X. Li, and Z. Liu, "Preparation of Gd_2O_2S:Pr scintillation ceramics by pressureless reaction sintering method," *Journal of Materials Science and Technology*, vol. 25, no. 2, pp. 254–258, 2009.

[5] E. I. Gorokhova, V. A. Demidenko, S. B. Eron'ko, O. A. Khristich, S. B. Mikhrin, and P. A. Rodnyĭ, "Spectrokinetic characteristics of the emission of Gd_2O_2S-Tb(Ce) ceramics," *Journal of Optical Technology*, vol. 72, no. 1, pp. 53–57, 2005.

[6] Y. Tian, W.-H. Cao, X.-X. Luo, and Y. Fu, "Preparation and luminescence property of Gd_2O_2S:Tb X-ray nano-phosphors using the complex precipitation method," *Journal of Alloys and Compounds*, vol. 433, no. 1-2, pp. 313–317, 2007.

[7] A. R. Faruqi and G. C. Tyrell, "Evaluation of gadolinium oxysulphide (P43) phosphor used in CCD detectors for electron microscopy," *Ultramicroscopy*, vol. 76, no. 1-2, pp. 69–75, 1999.

[8] C. Greskovich and S. Duclos, "Ceramic scintillators," *Annual Review of Materials Science*, vol. 27, no. 1, pp. 69–88, 1997.

[9] S. Som, A. Choubey, and S. K. Sharma, "Spectral and trapping parameters of Eu^{3+} in Gd_2O_2S nanophosphor," *Journal of Experimental Nanoscience*, vol. 10, no. 5, pp. 350–370, 2015.

[10] S. A. Osseni, S. Lechevallier, M. Verelst et al., "Gadolinium oxysulfide nanoparticles as multimodal imaging agents for T 2-weighted MR, X-ray tomography and photoluminescence," *Nanoscale*, vol. 6, no. 1, pp. 555–564, 2014.

[11] J. Huang, Y. Song, Y. Sheng et al., "Gd_2O_2S:Eu^{3+} and Gd_2O_2S:Eu^{3+}/Gd_2O_2S hollow microspheres: Solvothermal preparation and luminescence properties," *Journal of Alloys and Compounds*, vol. 532, pp. 34–40, 2012.

[12] F. Wang, B. Yang, J. Zhang, Y. Dai, and W. Ma, "Highly enhanced luminescence of Tb^{3+}-activated gadolinium oxysulfide phosphor by doping with Zn^{2+} ions," *Journal of Luminescence*, vol. 130, no. 3, pp. 473–477, 2010.

[13] C. He, Z. Xia, and Q. Liu, "Microwave solid state synthesis and luminescence properties of green-emitting Gd_2O_2S:Tb^{3+} phosphor," *Optical Materials*, vol. 42, pp. 11–16, 2015.

[14] F. Wang, D. Liu, B. Yang, and Y. Dai, "Characteristics and synthesis mechanism of Gd_2O_2S:Tb phosphors prepared by vacuum firing method," *Vacuum*, vol. 87, pp. 55–59, 2013.

[15] T. Hirai, T. Hirano, and I. Komasawa, "Preparation of Gd_2O_3:Eu^{3+} and Gd_2O_2S:Eu^{3+} particles using an emulsion liquid membrane system," *Journal of Colloid and Interface Science*, vol. 253, no. 1, pp. 62–69, 2002.

[16] K. Naghavi, E. Saion, K. Rezaee, and W. M. M. Yunus, "Influence of dose on particle size of colloidal silver nanoparticles synthesized by gamma radiation," *Radiation Physics and Chemistry*, vol. 79, no. 12, pp. 1203–1208, 2010.

[17] Y. Hu, J. Chen, X. Xue, and T. Li, "Synthesis of monodispersed single-crystal compass-shaped Mn_3O_4 via gamma-ray irradiation," *Materials Letters*, vol. 60, no. 3, pp. 383–385, 2006.

[18] A. Akhavan and E. Ataeevarjovi, "The effect of gamma irradiation and surfactants on the size distribution of nanoparticles based on soluble starch," *Radiation Physics and Chemistry*, vol. 81, no. 7, pp. 913-914, 2012.

[19] Y. Hu and J.-F. Chen, "Synthesis and characterization of semiconductor nanomaterials and micromaterials via gamma-irradiation route," *Journal of Cluster Science*, vol. 18, no. 2, pp. 371–387, 2007.

[20] S. Sharin, I. A. Rahman, A. F. Ahmad et al., "Reduction of graphene oxide to graphene by using gamma irradiation," *Malaysian Journal of Analytical Sciences*, vol. 19, no. 6, pp. 1223–1228, 2015.

[21] J. Lian, X. Sun, J.-G. Li, and X. Li, "Synthesis, characterization and photoluminescence properties of $(Gd_{0.99}, Pr_{0.01})_2O_2S$ submicrophosphor by homogeneous precipitation method," *Optical Materials*, vol. 33, no. 4, pp. 596–600, 2011.

[22] L. Hu, B. Yan, J. Zhang, and X. Wang, "The phosphorescent properties of Er^{3+} in Gd_2O_2S by two-step absorption," *Journal of Physics D: Applied Physics*, vol. 40, no. 23, pp. 7519–7522, 2007.

[23] R. K. Tamrakar, D. P. Bisen, and N. Brahme, "Comparison of photoluminescence properties of Gd_2O_3 phosphor synthesized by combustion and solid state reaction method," *Journal of Radiation Research and Applied Sciences*, vol. 7, no. 4, pp. 550–559, 2014.

[24] P. A. Rodnyi, "Energy levels of rare-earth ions in Gd_2O_2S," *Optics and Spectroscopy*, vol. 107, no. 2, pp. 270–274, 2009.

[25] Q. Mu and Y. Wang, "A simple method to prepare $Ln(OH)_3$ (Ln = La, Sm, Tb, Eu, and Gd) nanorods using CTAB micelle solution and their room temperature photoluminescence properties," *Journal of Alloys and Compounds*, vol. 509, no. 5, pp. 2060–2065, 2011.

[26] N. Akin, Y. Ozen, H. I. Efkere, M. Cakmak, and S. Ozcelik, "Surface structure and photoluminescence properties of AZO thin films on polymer substrates," *Surface and Interface Analysis*, vol. 47, no. 1, pp. 93–98, 2015.